No Precise Localization for Frb 150418: Claimed Radio Transient Is Agn Variability

Citation

Williams, P. K. G., and E. Berger. 2016. No Precise Localization for Frb 150418: Claimed Radio Transient Is Agn Variability. The Astrophysical Journal 821, no. 2: L22. doi:10.3847/2041-8205/821/2/l22.

Published Version

doi:10.3847/2041-8205/821/2/l22

Permanent link

http://nrs.harvard.edu/urn-3:HUL.InstRepos:30510187

Terms of Use

Share Your Story

The Harvard community has made this article openly available.
Please share how this access benefits you. Submit a story .

Accessibility

NO PRECISE LOCALIZATION FOR FRB 150418: CLAIMED RADIO TRANSIENT IS AGN VARIABILITY

P. K. G. Williams, E. Berger

Harvard-Smithsonian Center for Astrophysics, 60 Garden Street, Cambridge, MA 02138, USA

ABSTRACT

Keane et al. have recently claimed to have obtained the first precise localization for a Fast Radio Burst (FRB) thanks to the identification of a contemporaneous fading slow (∼week-timescale) radio transient. They use this localization to pinpoint the FRB to a galaxy at $z \approx 0.49$ that exhibits no discernible star formation activity. We argue that the transient is not genuine and that the host candidate, WISE J071634.59−190039.2, is instead a radio variable: the available data did not exclude this possibility; a random radio variable consistent with the observations is not unlikely to have a redshift compatible with the FRB dispersion measure; and the proposed transient light curve is better explained as a scintillating steady source, perhaps also showing an active galactic nucleus (AGN) flare, than a synchrotron-emitting blastwave. The radio luminosity of the host candidate implies that it is an AGN and we present new late-time Very Large Array observations showing that the galaxy is indeed variable at a level consistent with the claimed transient. Therefore the claimed precise localization and redshift determination for FRB 150418 cannot be justified.

Keywords: galaxies: active — intergalactic medium — radio continuum: general — scattering

1. INTRODUCTION

The origin of Fast Radio Bursts (FRBs; Lorimer et al. 2007) remains unknown, with both Galactic and extragalactic scenarios proposed (*e.g.*, Falcke & Rezzolla 2013; Loeb et al. 2014; Zhang 2014). The SUrvey for Pulsars and Extragalactic Radio Bursts (SUPERB) project has recently claimed to have obtained the first precise localization for an FRB by identification of an associated radio transient that faded over the course of six days (Keane et al. 2016). This transient was located in a seemingly passive elliptical galaxy at $z = 0.492 \pm 0.008$, a phenomenology which they argued to be consistent with the possible origin of (at least some) FRBs in compact object mergers (*e.g.*, Zhang 2014). This would be a truly exciting discovery, confirming the cosmological origin of (at least some) FRBs and hence also their extreme physics, their utility as a probe of the intergalactic medium (*e.g.*, McQuinn 2014), and the possibility that FRBs may be prompt, localizable electromagnetic tracers of gravitational-wave events (Abbott et al. 2016). The claimed localization of FRB 150418 has already been used to investigate the properties of its progenitor system (Wang et al. 2016; Zhang 2016) and place limits on the equivalence principle (Tingay & Kaplan 2016) and the mass of the photon (Bonetti et al. 2016).

Here we argue that the properties of the long-term radio emission from the proposed host point to a different and more mundane interpretation: that the observed variable radio emission is instead due to AGN activity, and that the variable emission and galaxy are not necessarily related to FRB 150418. Reasons to doubt the association (Section 2) include failure to exclude variable radio emission as a potential origin of the signal and the disagreement between the proposed transient light curve and synchrotron blastwave models, which are used to describe all confirmed classes of extragalatic radio transients. We also show that the agreement between the host candidate redshift and the dispersion measure (DM) of FRB 150418 is not unlikely, if the host candidate was selected based on short-timescale radio variability. We argue that the host candidate's quiescent radio luminosity implies that it hosts an AGN (Section 3) and present new data that we obtained with the Karl G. Jansky Very Large Array (VLA) demonstrating that it is indeed a variable radio source, attaining flux densities comparable to those attributed to the proposed radio transient (Section 4). In Section 5 we conclude that while other lines of evidence suggest an extragalactic origin for at least some FRBs (Masui et al. 2015), that currently available for FRB 150418 is unpersuasive.

The FRB 150418 host galaxy candidate is robustly detected in AllWISE imagery and is cataloged in the AllWISE Data Release as WISE J071634.59−190039.2. Hereafter we refer to it as WISE 0716−19.

2. REASONS TO DOUBT ASSOCIATION OF FRB 150418 AND WISE 0716−19

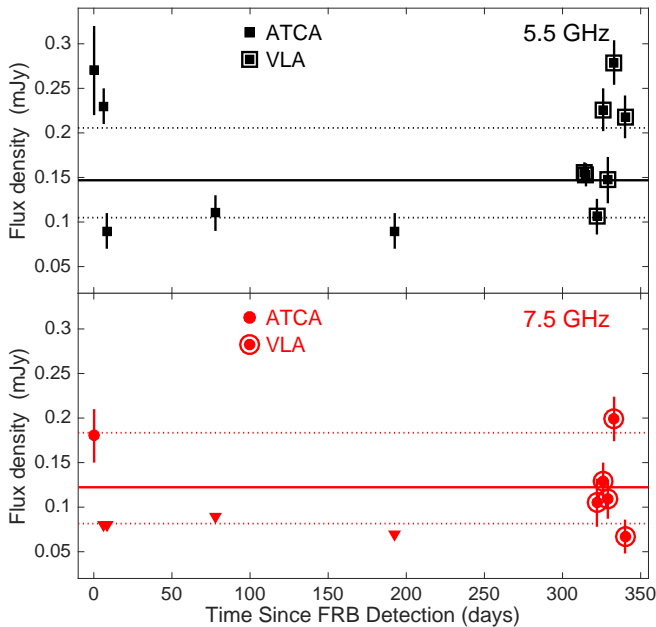Keane et al. (2016) followed up the detection of

pwilliams@cfa.harvard.edu

Figure 1. Radio light curve of WISE 0716−19 at 5.5 and 7.5 GHz (black and red, respectively) from VLA and ATCA (points with and without outlines, respectively). The ATCA data are from Keane et al. (2016). Each panel shows the best-fit model of a steady source affected by scintillation (Section 2.3), with the dotted lines showing the range of flux variation expected from refractive scintillation. The first two VLA epochs did not obtain data at 7.5 GHz and have been averaged together for clarity.

FRB 150418 with radio observations at several frequencies using several different telescopes. They achieved five detections of WISE 0716−19 with the Australia Telescope Compact Array (ATCA) at 5.5 GHz and one at 7.5 GHz; observations at other frequencies resulted in nondetections. We reproduce the ATCA data in Figure 1 using the measurements provided in Extended Data Table 1 of Keane et al. (2016), combining them with our new observations (Section 4). Here and below, we take the time of each observation to be its midpoint as computed by offsetting its tabulated start time by half of its duration. We compute $\Delta t = \mathrm{MJD} - 57130.19$ to express the approximate time after FRB 150418 in days. We do not apply barycentric or timescale corrections, which are not relevant to our analysis. There is a discrepancy between the Keane et al. (2016) table and their Figure 2: the table incorrectly lists the fourth ATCA epoch as occurring on 2015 June 4 when it should be 2015 July 4 (S. Johnston, 2016, priv. comm.).

In this section we provide several *a priori* reasons to doubt the association between FRB 150418 and WISE 0716−19.

2.1. *Failure to exclude coincident variable source*

The analysis of Keane et al. (2016) examines the probability of the chance discovery of an unassociated radio transient in their search field, but not the probability of the chance discovery of a variable radio source. The odds of the latter are non-negligible, as implied by the presence of a second compact variable radio source within the Parkes beam (Keane et al. 2016). The five detections of the ATCA light curve of WISE 0716−19 are insufficient to reject the possibility that it is a variable radio source, as demonstrated empirically by our new data showing that it in fact is one (Section 4).

Precise statements regarding the probability of chance detection of a candidate matching the characteristics reported by Keane et al. (2016) cannot be made without information regarding the total number of FRB localization regions searched by the SUPERB project and the process by which candidate transients were filtered, which is not currently available. However, in a catalog of 3652 compact sources brighter than ∼0.1 mJy at 3 GHz produced for the Caltech-NRAO Stripe 82 Survey pilot (CNSSp), Mooley et al. (2016) find that $3.9^{+0.5}_{-0.9}\%$ of them are variable at the >30% level. They only classified two sources as transients, implying that variables outnumber transients by a factor of ≈70 and that the "headline" chance coincidence probability of <0.1% reported by Keane et al. (2016) may be underestimated by a comparable amount. More generally, studies in which the analysis performed depends on the data taken will inevitably yield overconfident significance metrics due to the "garden of forking paths" effect (Gelman & Loken 2014).

Furthermore, the probability of a radio variable masquerading as a radio transient in the particular data set reported by Keane et al. (2016) may be even higher. Ofek et al. (2011) used the VLA to search a total area of 2.66 deg² for radio transients and variables. They find that 30% (30 out of 98) of sources brighter than 1.5 mJy at 5 GHz are variable at the 4σ level. Given the three radio sources with $S_\nu \gtrsim 0.1$ mJy detected in our VLA imaging (Section 4), which has a position and total area close to that of the Parkes search area, the expected number of radio variables in the field is therefore of order unity. Using the deep 5 GHz source counts of Fomalont et al. (1991), ∼16 sources brighter than 0.1 mJy are expected to be found in each Parkes beam. The typical Parkes search area may therefore host multiple variable radio sources.

Ofek et al. (2011) note that the rate of variables found in their survey is higher than comparable surveys and attribute this to their choice of observing frequency, the short averaging times of their observations, and the low Galactic latitude ($b \sim 6$–$8°$) of their survey. All of these

factors apply to the observations of Keane et al. (2016), with WISE 0716−19 being found at $b \sim -3.2°$. The correlation between low Galactic latitude and increased incidence of variability is well established and is due at least in part to higher levels of refractive scintillation through the denser ISM (Section 2.3; Spangler et al. 1989; Rickett 1990), implying that the increase in the number of variable sources is not only due to foreground objects.

2.2. *Significance of host galaxy redshift*

It may be argued that the agreement between the redshift of WISE 0716−19 and the DM of FRB 150418, given standard cosmological assumptions, supports the conclusion that the two are associated. Here we demonstrate that consistency between these is not unlikely even if the FRB and galaxy are unrelated.

We performed a Markov Chain Monte Carlo (MCMC) simulation to characterize the host galaxy redshifts that would have been found to be consistent with the DM of FRB 150418, given the assumptions made by Keane et al. (2016)[1]. The parameters are summarized in Table 1; the model is defined by Equation 1 and the surrounding discussion in Keane et al. (2016). We add a small (1%) uncertainty on the fraction of baryons contained in the intergalactic medium (IGM). Using a likelihood defined by the measured FRB DM and the priors listed in Table 1, we sampled from the posterior using the emcee package (Foreman-Mackey et al. 2013), which implements the Goodman & Weare (2010) affine-invariant sampling algorithm. We used 256 walkers divided into 8 independent groups each taking 8192 steps, thinning by a factor of 16 and discarding the first half of the samples from each walker. The mean proposal acceptance fraction was 41%, and there were in total ∼8500 independent samples of the redshift z, accounting for the estimated chain autocorrelation length of ∼6 samples after thinning. The $\hat{R}$ convergence criterion for the redshift parameter reached 1.08, implying good convergence (Gelman et al. 2013).

Figure 2 shows the redshift posterior samples marginalized over all other parameters. Given the model and data, host galaxy redshifts in the range 0.42–0.65 can be judged consistent with the measured DM of FRB 150418 at the 1σ level. The true range of host redshifts consistent with the data is broader than this — and our analysis is thus conservative — even if the assumption of an extragalactic origin is maintained, because other DM models are valid. For example, if, as we argue, the elliptical galaxy is not associated with FRB 150418 and the true

Figure 2. Posterior distribution of redshifts consistent with the observed DM of FRB 150418, from MCMC analysis using the nearly same model and uncertainties as Keane et al. (2016) (Section 2.2). The vertical axis is in units of probability per unit redshift so that the area under the curve is unity. Host galaxy redshifts in the range 0.42–0.65 are consistent with the data at the 1σ level, given the FRB DM and adopted model.

host is allowed to be a spiral rather than elliptical galaxy, its DM contribution could be significantly larger than the value assumed in the present model, broadening the distribution of allowed redshifts to include lower values.

Radio AGN are generally found at redshifts comparable to those allowed by the FRB DM measurement (*e.g.*, Condon et al. 1998). In its unbiased search for radio variables and transients, the CNSSp discovered 142 such objects in observations at 2–4 GHz. Of the 35 variables with variability timescales less than 1 week, there are 13 measured redshifts, ranging from 0.15 to 0.84 with a mean of 0.45. We further note that 90% (32/35) of these variables are classified as AGN. Of the full sample of CNSSp variables with redshift measurements, 22% (15/69) and 41% (28/69) are within the 1σ and 2σ limits of the posterior, respectively. A radio source selected on the basis of its variability is therefore not unlikely to have a redshift compatible with the DM of FRB 150418.

2.3. *Light curve of proposed transient and scintillation*

The only confirmed slowly-evolving extragalactic radio transients are synchrotron-emitting blastwaves, which exhibit a clear relationship between evolutionary timescale and luminosity (Metzger et al. 2015). From the observed flux of $F_\nu(5.5 \text{ GHz}) \sim 0.27$ mJy at a mid-point of $\Delta t = 0.2$, and assuming expansion at $v \approx c$ we infer a brightness temperature of $T_B \approx 5 \times 10^{15}$ K, which clearly requires relativistic expansion, with an inferred Lorentz factor of $\Gamma \approx 6$ to avoid the inverse Compton catastrophe limit of $T_B \approx 10^{12}$ K. Thus, if the observed emission is due to a synchrotron-emitting blastwave, it will obey

---

[1] We take this approach, rather than considering the likelihood that the the FRB DM would be found to be consistent with the host galaxy redshift, because the latter approach requires assumptions about the underlying distribution of FRB DMs, which is not well-constrained, as well as speculation as to what DM model would have been adopted by Keane et al. (2016) had a different DM been measured.
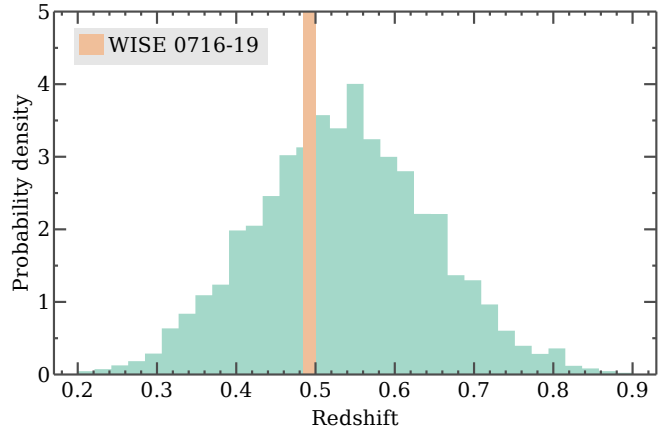
Table 1. Parameters of model used in DM MCMC analysis

Parameter	Symbol	Units	Prior
Host galaxy redshift	z	—	$U(10^{-4}, 20)$[a]
Host galaxy DM	$\mathrm{DM_{host}}$	$\mathrm{cm^{-3}\ pc}$	$N(37, 37 \times 20\%)$[b]
Milky way DM	$\mathrm{DM_{MW}}$	$\mathrm{cm^{-3}\ pc}$	$N(188.5, 188.5 \times 20\%)$
Milky way halo DM	$\mathrm{DM_{halo}}$	$\mathrm{cm^{-3}\ pc}$	$N(30, 5)$[c]
Dark energy content of universe	Ω_Λ	—	$N(0.721, 0.025)$
Matter content of universe	Ω_m	—	$N(0.233, 0.023)$
Baryonic content of universe	Ω_b	—	$N(0.0463, 0.0024)$
Present-day Hubble parameter	H_0	$\mathrm{km\ s^{-1}\ Mpc^{-1}}$	$N(70.0, 2.2)$
Fraction of baryons in IGM	f_{IGM}	—	$N(0.90, 0.01)$

[a]Denotes a uniform distribution between the specified bounds.

[b]Denotes a normal distribution with the specified mean and standard deviation.

[c]Uncertainty estimated from Figure 2 of Dolag et al. (2015).

the basic relativistic afterglow evolution of GRBs (Sari et al. 1998, 1999; Granot & Sari 2002). The synchrotron emission model is characterized by three break frequencies — self-absorption (ν_a), peak (ν_m) and cooling (ν_c) – and an overall flux density normalization ($F_{\nu,m}$). These parameters in turn determine the physical properties of the blastwave: isotropic kinetic energy ($E_{K,\mathrm{iso}}$), density (n), and fractions of post-shock energy in the relativistic electrons (ϵ_e) and magnetic fields (ϵ_B). The power law distribution of the relativistic electrons is further determined by an index, p, such that $N(\gamma) \propto \gamma^{-p}$ at $\gamma \geq \gamma_m$. This model has been used to study GRB afterglows for the past 15 years.

Compact radio sources — including both GRB afterglows and AGN jets — are furthermore subject to interstellar scintillation (ISS) by the interstellar medium of the Milky Way (Spangler et al. 1989; Rickett 1990). For the low Galactic latitude sight-line to FRB 150418 the scattering measure is large, $\log(\mathrm{SM}) \approx -2.4$ (Cordes & Lazio 2002), and hence frequencies below $\nu_0 \approx 30$ GHz are subject to strong scintillation. We do not consider diffractive ISS to be important because the coherence bandwidth is $\delta\nu/\nu \approx (\nu/\nu_0)^{17/5} \approx 20$ MHz, much narrower than the GHz bandwidth of the ATCA and VLA observations. However, strong refractive interstellar scintillation (RISS) is expected, with a modulation index (rms fractional variation) of $\sim$0.4 and 0.5 at 5.5 and 7.5 GHz, respectively. This level of variability will be present for any source that is compact relative to the characteristic RISS angular size θ_s. Taking a scattering screen distance of 1 kpc, we find $\theta_s \sim 50$ μas at 5.5 GHz (Walker 1998), corresponding to a linear scale of $\sim$0.2 pc at the redshift of WISE 0716−19. In our modeling of the radio emission below we account for the effect of RISS by adding the expected modulation of the model light curves in quadrature to the measurements uncertainties.

We model the radio light curve with the afterglow model

of Granot & Sari (2002) using standard parameters for GRB afterglows: $\epsilon_e = 0.1$, $\epsilon_B = 0.01$, and $p = 2.5$. We note that the ATCA data indicate that $\nu_a < 5.5$ GHz, and moreover the radio data do not constrain ν_c, which is typically located in the optical to X-ray regime. As a result, the model light curves are degenerate with respect to our choice of ϵ_e and ϵ_B, with the inferred values of $E_{K,\mathrm{iso}}$ and n changing with the choice of values, but the light curves (and hence the quality of fit) remaining unchanged. We tested models with values of ϵ_e and ϵ_B varying between 0.1 and 10^{-6}, and find identical χ_r^2 values. We use models with both a spherical geometry and a jet, leaving the blastwave kinetic energy and the density as free parameters, as well as the jet opening angle in the latter model. We also include a constant term with a flux density of 0.09 mJy at 5.5 GHz and 0.065 mJy at 7.5 GHz to represent the steady component detected in the ATCA data at $\Delta t \gtrsim 8$; our 7.5 GHz steady component agrees with the ATCA upper limits and assumes a ν^{-1} spectrum for this component. The best-fit models are shown in Figure 3. Both models provide a poor fit to the data, with $\chi_r^2 \approx 8.0$ (spherical; 8 degrees of freedom) and ≈ 8.8 (jet; 7 degrees of freedom) assuming no RISS. The inclusion of RISS leads to $\chi_r^2 \approx 1.5$ and ≈ 1.6, respectively. In this latter case, we assume that the steady component scintillates as well; if it does not (i.e., is not compact), the χ_r^2 values increase since the scintillation-induced uncertainty in the model is lower.

We next compare these models to a simple steady source which is modulated purely by RISS. In this case we find a mean flux density of 0.135 mJy at 5.5 GHz and 0.100 mJy at 7.5 GHz (i.e., assuming a ν^{-1} spectrum). This simpler model results in $\chi_r^2 \approx 6.4$ (8 degrees of freedom) when ignoring RISS and $\chi_r^2 \approx 1.1$ when including RISS.

The synchrotron models are challenged by the data at $\Delta t < 8$, which show a rapid evolution in spectral slope that is not expected from a synchrotron blastwave. More
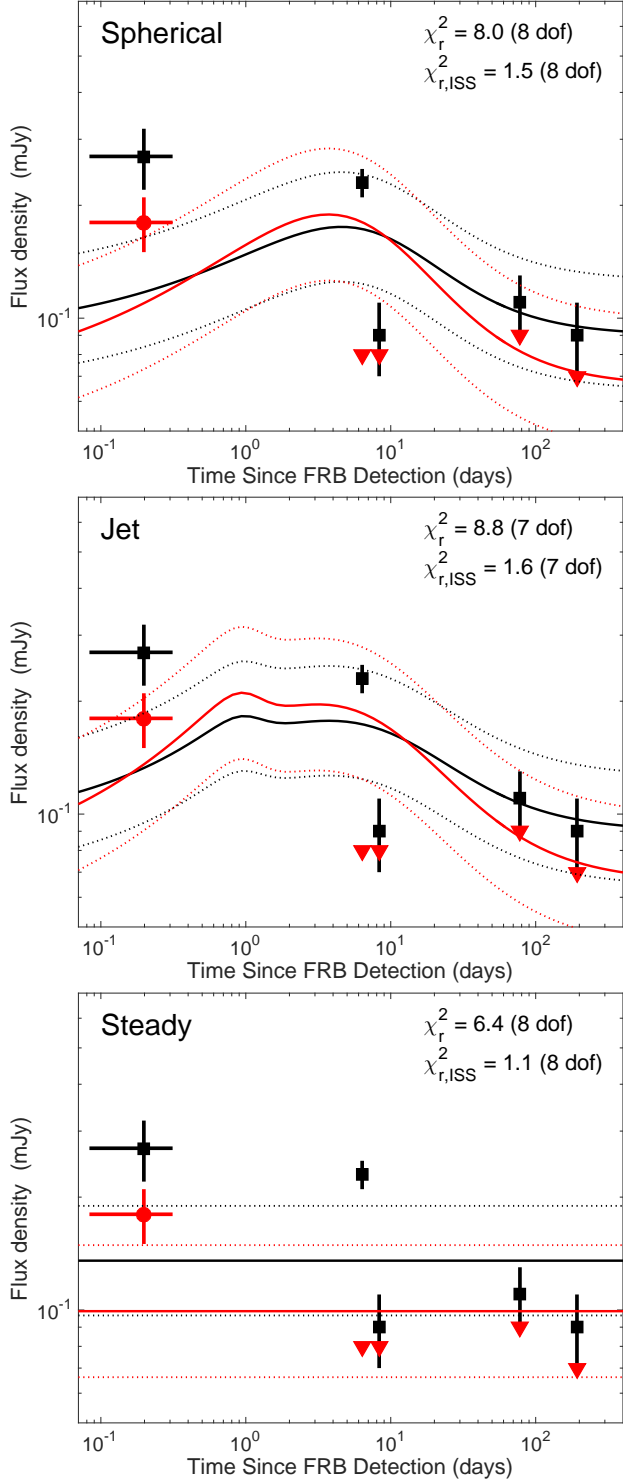
Figure 3. Three theoretical models fit to the ATCA data: synchrotron blastwaves with spherical (top) and jetted (middle) geometries, and a steady source (bottom). Colors and symbols are as in Figure 1, with the horizontal error bar on the first point indicating the duration of the relevant observation. Regardless of whether RISS is assumed to play a role or not, the constant model is more consistent with the data than the forward shock afterglow models.

specifically, while the spectral indices of the first and third epochs of ATCA observations are not atypical, the second epoch implies an exceptionally steep $\alpha \lesssim -3.4$ between 5.5 and 7.5 GHz. This variation may be compatible with RISS, which has a correlation bandwidth $\Delta\nu/\nu \sim 1$. Recent observations suggest that flares in faint AGN can result in rapid spectral evolution: α evolved from -1.7 to $+0.4$ over 15 days in a source (VTC225411$-$010651) found in the CNSSp. We speculate that this mechanism is at work in this case as well.

Thus, while Keane et al. (2016) (and similarly Zhang 2016) claim that the post-FRB radio data are consistent with a short GRB afterglow, the data actually favor other interpretations. The best formal fit to the data is of a model of a steady source modulated by the inevitable strong refractive scintillation. The rapid spectral evolution observed at $\Delta t < 8$ may suggest the presence of an AGN flare. This spectral evolution is inconsistent with a synchrotron blastwave, such as a short GRB afterglow.

3. ALTERNATE INTERPRETATION: AGN VARIABILITY

In the interpretation of Keane et al. (2016), the three 5.5 GHz ATCA data points at $\Delta t \sim (8, 49, 193)$ are due to quiescent radio emission at a level of 0.097 ± 0.012 mJy, where we have simply taken the weighted mean of the three measurements. At the redshift of the galaxy this corresponds to a radio spectral luminosity of $\sim 9 \times 10^{29}$ erg s^{-1} Hz^{-1}. Using the standard relations of Yun & Carilli (2002), the star formation rate (SFR) inferred from the radio spectral luminosity is $\sim 10^2$–10^3 M$_\odot$ yr^{-1}, orders of magnitude higher than the value of ≤ 0.2 M$_\odot$ yr^{-1} that Keane et al. (2016) infer from Hα in the optical spectrum of the galaxy. Thus, the origin of the quiescent radio emission is not star formation activity.

As argued by Brown et al. (2011) in their investigation of the radio emission from bright early-type galaxies comparable to WISE 0716$-$19, if the galaxy's bright radio emission is not due to star formation, the alternative source is AGN activity. This is immediately worrisome because AGN are both intrinsically and extrinsically variable (Section 2.3) and can thus falsely appear as transient radio sources. While the spectrum of the host does not show clear quasar features, spectra of matched SDSS-FIRST sources show that optical signatures of AGN activity are frequently not visible in spectra of luminous early-type galaxies with radio emission similar to WISE 0716$-$19 (Ivezić et al. 2002). Studies of radio-loud AGN demonstrate that the WISE colors are consistent with AGN activity (Gürkan et al. 2014).

4. VLA FOLLOW-UP OBSERVATIONS

To test the AGN hypothesis, we are obtaining follow-up observations with the VLA using Director's Discretionary

time. Here we present the first results from our program (number VLA/16A-431).

Table 2 summarizes our observations and the results of our analysis. In all cases, the bandpass and flux density calibrator was 3C 147, and the gain and phase calibrator was the nearby ($\sim5°$ distant) source PKS 0733−17. A standard continuum wideband correlator setup was used, with 512 channels of 2 MHz width correlated around center frequencies of 5.5 GHz and 7.5 GHz, the same as used by Keane et al. (2016). The first two epochs did not obtain data at the higher frequency. The correlator dump time was 5 s. Radio-frequency interference was flagged automatically using the aoflagger tool, which provides post-correlation (Offringa et al. 2010) and morphological (Offringa et al. 2012) algorithms for identifying interference. After applying standard calibration techniques in CASA (McMullin et al. 2007), we imaged different portions of the data using the CASA imager with $1''$ square pixels, 128 w-projection planes (Cornwell et al. 2005), multi-frequency synthesis (Sault & Wieringa 1994), and CASA's multi-frequency clean algorithm.

In the images we detect an unresolved source coincident with WISE 0716−19. In a stack of all of the data, the position is RA = 07:16:34.64, Dec. = −19:00:40.7, with an uncertainty of 0.4 arcsec; this may be compared with the AllWISE position, RA = 07:16:34.598, Dec. = −19:00:39.26; and the ATCA position reported by Keane et al. (2016), RA = 07:17:34.6, Dec. = −19:00:40, where the uncertainties on these are ~0.1 and ~1 arcsec, respectively. The radio positions are consistent with emission from the centroid of the galaxy.

We measured the source's flux density by least-squares parameter fitting of the image data and report the results in Table 2, where the flux density uncertainties are derived from the least-squares covariance matrix. The minimum and maximum 5.5 GHz flux densities we observe are 0.105 ± 0.021 and 0.279 ± 0.025 mJy, consistent with the radio transient proposed by Keane et al. (2016). We investigated the short-timescale variability of the radio source using the visibility-based technique described in Williams et al. (2013), finding no evidence of variability on the half-hour time scales of the individual epochs.

There are two other sources in the VLA field of view that are detectable in our brief observations. These are found at RA = 07:16:39.4, Dec. = −18:56:30 and RA = 07:16:04.0, Dec. = −19:00:16, separated from the pointing center by 1.1 and 1.8 times the half-width at half-power of the VLA primary beam at 5.5 GHz, respectively. Our flux density measurements of these sources vary at the 10% and 20% levels, respectively, which is about twice the level expected from noise. The variations among the three sources are inconsistent with an error in the data's overall gain calibration, and extensive checking of the data reveals no worrisome artifacts. We speculate that the variation we observe is due to a combination of pointing errors and possibly intrinsic variability; one of these sources may be the additional radio variable reported by Keane et al. (2016).

The typical synthesized beam in the ATCA observations was $10'' \times 2''$ with North-South elongation (S. Johnston, 2016, priv. comm.), comparable to that in our VLA observations. Combined with the fact that the source appears unresolved in both data sets, we infer that a potential systematic flux density difference due to the "resolving out" of flux by interferometers with different configurations is small. Regardless, any such systematic difference cannot be responsible for the variation seen in the VLA data set.

5. CONCLUSIONS

We have pursued three lines of argument against the association between FRB 150418 and WISE 0716−19 proposed by Keane et al. (2016). First, the possibility that WISE 0716−19 is a radio variable was not sufficiently excluded. Second, the agreement between the DM of the FRB and the redshift of the candidate host galaxy is not surprising if the host is a randomly-selected radio variable. Third, the radio light curve of the proposed transient is better explained as a steady source affected by strong interstellar scintillation, possibly also showing an AGN flare, than as any of the classes of confirmed extragalactic radio transients.

We argue that the radio luminosity of WISE 0716−19 indicates that it is indeed a variable radio source, namely an AGN. Our new data confirm its variability and show that the galaxy's brightness can reattain the level attributed to a radio transient by Keane et al. (2016). The available evidence therefore cannot support the identification of WISE 0716−19 as the host galaxy of FRB 150418, negating the claimed localization and definitive cosmological origin of the event.

Table 2. Parameters of VLA observations

Parameter	Units	Epoch						
		Feb. 27	Feb. 28	Mar. 05	Mar. 08	Mar. 11	Mar. 16	Mar. 23
Observation start time	MJD	57445.028	57446.018	57452.015	57456.006	57458.989	57463.972	57470.967
Observation duration	minutes	90	90	30	30	30	30	30
5.5 GHz:								
Synthesized beam size	arcsec	8.6×3.3	8.9×3.3	9.7×3.2	9.6×3.2	10.4×3.2	11.9×3.2	9.8×3.6
Calibrator flux density[a]	mJy	1.197 ± 0.002	1.187 ± 0.002	1.184 ± 0.004	1.202 ± 0.003	1.209 ± 0.003	1.183 ± 0.004	1.164 ± 0.005
RMS at phase center	mJy	0.0077	0.0091	0.015	0.017	0.018	0.018	0.015
WISE 0716−19 flux density	mJy	0.156 ± 0.011	0.153 ± 0.013	0.105 ± 0.021	0.225 ± 0.024	0.147 ± 0.026	0.279 ± 0.025	0.218 ± 0.024
7.5 GHz:								
Synthesized beam size	arcsec	$\cdots$	$\cdots$	7.0×2.2	6.9×2.3	7.3×2.2	7.7×2.1	7.0×2.5
Calibrator flux density[a]	mJy	$\cdots$	$\cdots$	0.894 ± 0.007	0.915 ± 0.004	0.933 ± 0.004	0.898 ± 0.006	0.877 ± 0.007
RMS at phase center	mJy	$\cdots$	$\cdots$	0.019	0.015	0.016	0.017	0.014
WISE 0716−19 flux density	mJy	$\cdots$	$\cdots$	0.103 ± 0.027	0.132 ± 0.021	0.109 ± 0.022	0.199 ± 0.025	0.067 ± 0.019
WISE 0716−19 spectral index		$\cdots$	$\cdots$	-0.1 ± 1.1	-1.8 ± 0.7	-1.0 ± 0.9	-1.1 ± 0.5	-3.9 ± 1.1

[a]Does not include systematic errors on the absolute flux density scale.

Facilities: Karl G. Jansky Very Large Array

Software: CASA, emcee

REFERENCES

Abbott, B. P., Abbott, R., Abbott, T. D., et al. 2016, Phys. Rev. Lett., 116, 061102

Bonetti, L., Ellis, J., Mavromatos, N. E., et al. 2016, Preprint, arxiv:1602.09135

Brown, M. J. I., Jannuzi, B. T., Floyd, D. J. E., & Mould, J. R. 2011, ApJL, 731, L41

Condon, J. J., Cotton, W. D., Greisen, E. W., et al. 1998, AJ, 115, 1693

Cordes, J. M., & Lazio, T. J. W. 2002, ArXiv Astrophysics e-prints, astro-ph/0207156

Cornwell, T. J., Golap, K., & Bhatnagar, S. 2005, in Astronomical Society of the Pacific Conference Series, Vol. 347, Astronomical Data Analysis Software and Systems XIV, ed. P. Shopbell, M. Britton, & R. Ebert

Dolag, K., Gaensler, B. M., Beck, A. M., & Beck, M. C. 2015, MNRAS, 451, 4277

Falcke, H., & Rezzolla, L. 2013, A&A, 562, 137

Fomalont, E. B., Windhorst, R. A., Kristian, J. A., & Kellerman, K. I. 1991, AJ, 102, 1258

Foreman-Mackey, D., Hogg, D. W., Lang, D., & Goodman, J. 2013, PASP, 125, 306

Gelman, A., Carlin, J. B., Stern, H. S., et al. 2013, Bayesian Data Analysis, 3rd edn. (CRC Press)

Gelman, A., & Loken, E. 2014, American Scientist, 102, 460

Goodman, J., & Weare, J. 2010, Communications in Applied Mathematics and Computational Science, 5, 65

Granot, J., & Sari, R. 2002, ApJ, 568, 820

Gürkan, G., Hardcastle, M. J., & Jarvis, M. J. 2014, MNRAS, 438, 1149

Ivezić, v., Menou, K., Knapp, G. R., et al. 2002, AJ, 124, 2364

Keane, E. F., Johnston, S., Bhandari, S., et al. 2016, Natur, 530, 453

Loeb, A., Shvartzvald, Y., & Maoz, D. 2014, MNRAS Lett., 439, 46

Lorimer, D. R., Bailes, M., McLaughlin, M. A., Narkevic, D. J., & Crawford, F. 2007, Science, 318, 777

Masui, K., Lin, H.-H., Sievers, J., et al. 2015, Natur, 528, 523

McMullin, J. P., Waters, B., Schiebel, D., Young, W., & Golap, K. 2007, in Astronomical Society of the Pacific Conference Series, Vol. 376, Astronomical Data Analysis Software and Systems XVI, ed. R. A. Shaw, F. Hill, & D. J. Bell, 127

McQuinn, M. 2014, ApJL, 780, L33

Metzger, B. D., Williams, P. K. G., & Berger, E. 2015, ApJ, 806, 224

Mooley, K. P., Hallinan, G., Bourke, S., et al. 2016, ApJ, 818, 105

Ofek, E. O., Frail, D. A., Breslauer, B., et al. 2011, ApJ, 740, 65

Offringa, A. R., de Bruyn, A. G., Biehl, M., et al. 2010, MNRAS, 405, 155

Offringa, A. R., van de Gronde, J. J., & Roerdink, J. B. T. M. 2012, A&A, 539, A95

Rickett, B. J. 1990, ARA&A, 28, 561

Sari, R., Piran, T., & Halpern, J. P. 1999, ApJL, 519, L17

Sari, R., Piran, T., & Narayan, R. 1998, ApJL, 497, L17

Sault, R. J., & Wieringa, M. H. 1994, A&AS, 108, 585

Spangler, S., Fanti, R., Gregorini, L., & Padrielli, L. 1989, A&A, 209, 315

Tingay, S. J., & Kaplan, D. L. 2016, ApJL submitted, arxiv:1602.07643

Walker, M. A. 1998, Monthly Notices of the Royal Astronomical Society, 294, 307

Wang, J.-S., Yang, Y.-P., Wu, X.-F., Dai, Z.-G., & Wang, F.-Y. 2016, Preprint, arxiv:1603.02014

Williams, P. K. G., Berger, E., & Zauderer, B. A. 2013, ApJL, 767, L30

Yun, M. S., & Carilli, C. L. 2002, ApJ, 568, 88

Zhang, B. 2014, ApJL, 780, L21

—. 2016, ArXiv Astrophysics e-prints, 1602.08086